Toxicology in Vitro 26 (2012) 1030–1039

Contents lists available at SciVerse ScienceDirect

Toxicology in Vitro

journal homepage: www.elsevier.com/locate/toxinvit

# Isatin-3-N$^4$-benzilthiosemicarbazone, a non-toxic thiosemicarbazone derivative, protects and reactivates rat and human cholinesterases inhibited by methamidophos in vitro and in silico

Rômulo Pillon Barcelos [a], Rafael de Lima Portella [a], Thiago Henrique Lugokenski [a], Edovando José Flores da Rosa [a], Guilherme Pires Amaral [a], Luiz Filipe Machado Garcia [a], Leandro Bresolin [b], Vanessa Carratu [b], Félix Alexandre Antunes Soares [a,*], Nilda Berenice de Vargas Barbosa [a]

[a] Departamento de Química, Centro de Ciências Naturais e Exatas, Universidade Federal de Santa Maria, Campus UFSM, 97105-900 Santa Maria, RS, Brazil
[b] Departamento de Química, Fundação Universidade de Rio Grande, Campus Carreiros, Rio Grande, RS, Brazil

ARTICLE INFO

*Article history:*
Received 8 February 2012
Accepted 10 April 2012
Available online 20 April 2012

*Keywords:*
Antioxidant
Cholinesterases
Molecular docking
Thiosemicarbazones
Methamidophos

ABSTRACT

Organophosphates (OPs), which are widely used as pesticides, are acetylcholinesterase (AChE) and butyrylcholinesterase (BChE) inhibitors. The inactivation of AChE results in the accumulation of acetylcholine at cholinergic receptor sites, causing a cholinergic crisis that can lead to death. The classical treatment for OP poisoning is administration of oximes, but these compounds are ineffective in some cases. Here we determined whether the new compound isatin-3-N$^4$-benzilthiosemicarbazone (IBTC), which in our previous study proved to be an antioxidant and antiatherogenic molecule, could protect and reactivate AChE and BChE. Toxicity of IBTC after subcutaneous injection in mice was measured using assays for oxidized dicloroflurescein (DCF), thiobarbituric acid reactive substances (TBARS), non-protein thiol (NPSH) levels, and catalase (CAT), sodium potassium ($Na^+/K^+$) ATPase, delta-aminolevulinic acid dehydratase (ALA-D), and glutathione peroxidases (GPx) enzyme activities. The cytotoxicity was evaluated and the enzymatic activity of cholinesterase was measured in human blood samples. Molecular docking was used to predict the mechanism of IBTC interactions with the AChE active site. We found that IBTC did not increase the amount of DCF-RS or TBARS, did not reduce NPSH levels, and did not increase CAT, ($Na^+/K^+$) ATPase, ALA-D, or GPx activities. IBTC protected and reactivated both AChE and BChE activities. Molecular docking predicted that IBTC is positioned at the peripheral anionic site and in the acyl binding pocket of AChE and can interact with methamidophos, releasing the enzyme's active site. Our results suggest that IBTC, besides being an antioxidant and a promising antiatherogenic agent, is a non-toxic molecule for methamidophos poisoning treatment.



## 1. Introduction

Organophosphates (OPs), which inhibit cholinesterase, have been widely used as pesticides and additives for lubricants and have been developed as warfare nerve agents (WHO, 1993). The toxic action of OPs is related to the binding of these compounds to the active site of the acetylcholinesterase enzyme (AChE; EC 3.1.1.7), thus inhibiting hydrolysis of the acetylcholine neurotransmitter (ACh) at central and peripheral synapses (Holmstedt, 1959; Taylor et al., 1995). The inactivation of AChE results in an accumulation of acetylcholine at cholinergic receptor sites and a cholinergic crisis that can lead to death, usually via respiratory failure due to paralysis of the diaphragm and intercostals muscles, as well as cerebral respiratory center depression and excessive bronchial secretion (Marrs, 1993).

The enzymes associated with antioxidant defense mechanisms are altered under the influence of pesticides, leading to an imbalance between generation of oxidant molecules and intracellular antioxidant systems (Banerjee et al., 1999), which may induce oxidative stress in rats (Gultekin et al., 2000; Gupta et al., 2001), mice (da Silva et al., 2006, 2008), and humans (Banerjee et al., 1999). Moreover, OPs cause lipid peroxidation in rat brains (Verma and Srivastava, 2001) and human erythrocytes (Gultekin et al., 2000). However, the exact mechanism by which OPs induce oxidative damage is not fully understood (Abdollahi et al., 2004).

Methamidophos (MAP) is an OP and a potent AChE inhibitor used to control insects that plague a variety of crops such as brassica, cotton, tobacco, sugar beet, lettuce, potatoes, and tree fruits (WHO, 1993). MAP is highly toxic to aquatic organisms (Tomlin, 1994) and mice (Zayed et al., 1984). It also has anticholinesterase

* Corresponding author. Tel.: +55 55 3220 9522.
*E-mail addresses:* felix_antunes_soares@yahoo.com.br, felix@ufsm.br (F.A.A. Soares).

0887-2333 
http://dx.doi.org/10.1016/j.tiv.2012.04.008

activity in humans (Worek et al., 2007, 2004). Acetylcholinesterase (AchE) inhibition by OPs can generally be reversed by treatment with oximes (Worek et al., 2004). However, there is a need for more efficient compounds with broader reactivation activity after exposure to different OPs and that are less toxic to humans.

The crystal structure of AChE (Bourne et al., 1995; Ekström et al., 2006; Kryger et al., 1998; Sussman et al., 1991) allows for detailed structural studies on ligand access to the enzyme's active center gorge and the steric constraints within the active center gorge that govern selectivity during reactivation (Ashani et al., 1995; Grosfeld et al., 1996; Kovarik et al., 2004; Wong et al., 2000). The orientation of the compound within the narrow confines of the gorge when the active serine is phosphorylated is an important determinant of the reactivation mechanism (Musilek et al., 2011). There are several in silico studies that illustrate the ability of this structural model to reliably predict molecular interactions.

There is considerable interest in thiosemicarbazones due to their wide pharmacological utility (Beraldo and Gambino, 2004) and versatility as ligands. They have recently been investigated as radical scavengers (Wada et al., 1994) and our previous study (Barcelos et al., 2011) revealed that a thiosemicarbazone derivate, isatin-3-$N^4$-benzilthiosemicarbazone (IBTC), is also effective as an antioxidant and antiatherogenic molecule. Although the use of thiosemicarbazone as an antiatherogenic molecule has been suggested previously (Barcelos et al., 2011), in vitro and in vivo toxicological screening is still needed.

Therefore, the aim of this study was to test the toxicological effects of IBTC, a thiosemicarbazone derivate, and to identify the effective concentration of IBTC for protecting and reactivating cholinesterases after exposure to MAP. In addition, any possible inhibitory effects of IBTC on the thiol-containing enzymes from the blood/liver and brain, namely delta-aminolevulinic acid dehydratase (ALA-D) and $Na^+/K^+$-ATPase, respectively, were also evaluated. Docking studies were carried out in silico to evaluate the minimal energy IBTC conformations in the active site of human AChE when the active site serine is phosphorylated by MAP.

## 2. Materials and methods

### 2.1. Synthesis of isatin-3-$N^4$-benzilthiosemicarbazone

The synthesis of isatin-3-$N^4$-benzilthiosemicarbazone (IBTC) was performed as described previously (Fonseca et al., 2010) and the chemical structure of IBTC is depicted in Fig. 1.

### 2.2. Chemical reagents

The reagents thiobarbituric acid (TBA), dicloroflouresceine diacetate (DCFH-DA), methyltetrazolium (MTT), ethylene glycol tetraacetic acid (EGTA), Ellman's reagent (5,5′-dithiobis-(2-nitrobenzoic acid) or DTNB), *N*,*N*,*N*′,*N*′-tetramethylbenzidine and ouabaine were supplied by Sigma–Aldrich Chemical Co. (St. Louis, MO); acetylthiocholine iodide supplied by Merck. The other used reagents were obtained from local suppliers.

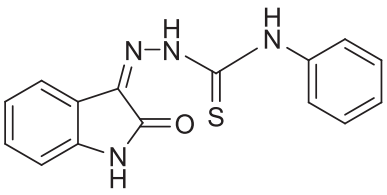


**Fig. 1.** Chemical structure of IBTC.

### 2.3. Separation of human red blood cells

Human red blood cells (RBC) were separated from heparinized blood that was drawn from a healthy donor. The blood was centrifuged at 2000 rpm for 10 min to separated the RBCs from plasma, then the RBCs were washed three times with phosphate-buffered saline (PBS) at pH 7.4.

### 2.4. Isolation of lymphocytes from human blood

Lymphocytes were isolated from human blood collected from a healthy donor with EDTA and separated on Ficoll–Histopaque density gradients as described previously (Böyum, 1968).

### 2.5. Cell culture

Cell culture Murine J774 macrophage-like cells were obtained from the American Type Culture Collection (ATCC, Rockville, MD, USA). These cells were maintained with Dulbecco's Modified Eagle Medium (DMEM) supplemented with 2 mM glutamine, 10 mM HEPES, 100 U/mL penicillin, 100 μg/mL streptomycin and 10% fetal bovine serum (FBS) in a 5% $CO_2$ humidified atmosphere at 37 °C.

### 2.6. Experimental animals

Untreated adult male swiss albino mice (25–30 g) were obtained from our own breeding colony. The animals were maintained in an air conditioned room (20–25 °C) under a 12 h light/dark cycle, and with water and food ad libitum. All the experimental procedures performed were conducted according to the guidelines of the Committee of Ethics in Research of the Federal University of Santa Maria, Brazil.

### 2.7. Animal treatment

Adult male swiss albino mice received a single subcutaneous injection of the IBTC dissolved in DMSO in different doses (1, 10, 50, 100, 250 or 500 mg/kg) ($n$ = 4 animals/dose). Control animals received DMSO at 5 mL/kg. To determine the potential lethality of the IBTC, animals were observed for up to 24 h after compound administration. $LD_{50}$ was calculated using "GraphPad Software" (GraphPad Software, San Diego, CA). After this period, animals were euthanized by cervical dislocation. The liver, kidney, heart and brain were quickly removed, placed on ice, and homogenized within 10 min, in 10 volumes of cold Tris 10 mM (pH 7.4). The homogenates were centrifuged at 4000*g* at 4 °C for 10 min to yield a low-speed supernatant fraction (S1) for each tissue that was used for ex vivo analysis.

### 2.8. Whole blood and blood components

Mice were euthanized and the whole blood was collected (cardiac puncture) in previously heparinized tubes and kept under refrigeration. Whole blood samples were precipitated with TCA 40% (1:1) and centrifuged (4000*g* at 4 °C for 10 min) in order to obtain the supernatant fraction that was used for non protein thiol measurement determination. Other heparinized blood samples were used for Delta Aminolevulinate Dehydratase (δ-ALA-D) activity measurement and other were centrifuged at 1000*g* at 4 °C for 10 min in order to obtain cellular blood fractions which were used for oxidized dicloroflouresceine and Delta Aminolevulinate Dehydratase (δ-ALA-D) activity measurement (Puntel et al., 2011).

### 2.9. Oxidized dicloroflurescein (DCF-RS) levels

DCF-RS levels were determined as an index of the peroxide production by the cellular components (Myhre et al., 2003). Aliquots cellular blood fraction (10 μL) or liver, kidney, heart and brain S1 (50 μL) were added to a medium containing Tris–HCl buffer (0.01 mM; pH 7.4) and DCFH-DA (7 μM). After DCFH-DA addition, the medium was incubated in the dark for 1 h until fluorescence measurement procedure (excitation at 488 nm and emission at 525 nm and both slit widths used were at 5 nm). DCF-RS levels were determined using a standard curve of DCF and the results were corrected by the protein content (Pérez-Severiano et al., 2004).

### 2.10. Thiobarbituric acid reactive substances (TBARS) levels

Analyses were performed in liver, kidney, heart and brain S1 samples according to the method described previously (Pérez-Severiano et al., 2004). Aliquots of 200 μL of liver, kidney, heart and brain S1 were added to color reaction. TBARS levels were measured at 532 nm using a standard curve of MDA and corrected by the protein content (Ohkawa et al., 1979).

### 2.11. Catalase (CAT)

The CAT enzyme activity was determined in liver, kidney and heart S1 according to the method proposed by Aebi H (Aebi, 1984). Briefly, S1 aliquot (50 μL) was added to a medium containing potassium phosphate buffer (50 mM; pH 7.4) and $H_2O_2$ (1 mM). The kinetic analysis of CAT was started after $H_2O_2$ addition and the color reaction was measured at 240 nm. One unit of the enzyme is considered as the amount which decomposes 1 μmol $H_2O_2$/min at pH 7.

### 2.12. Sodium potassium ($Na^+/K^+$) ATPase

The cerebral $Na^+/K^+$ATPase enzyme activity was determined in brain S1 samples according to the method proposed by Muszbek et al. (1977), with some modifications. Briefly, the aliquots of skeletal muscle S1 (20 μL) were added to a reaction medium containing NaCl (115 mM), $MgCl_2$ (2.5 mM), KCl (18 mM) and Tris–HCl buffer (45 mM and pH 7.4), with or without the $Na^+/K^+$ ATPase enzyme inhibitor ouabaine (5 μM). The method for ATPase activity measurement was based on the determination of the inorganic phosphate (Pi) released to the reaction medium by the hydrolysis of the ATP according to the method proposed by Atkinson A (Atkinson et al., 1973). The reaction was initiated with the addition of the substrate ATP (1.5 mM) to the reaction medium and was finished by the addition of the color reagent (1 mL) containing ammonium molibdate (2%), Triton-X 100 (5%) and $H_2SO_4$ 1.8 M (10%) after 15 min of incubation at 37 °C. The formed molibdate–Pi complexes were measured spectrophotometrically at 405 nm. Values were calculated in relation to a standard curve constructed with Pi at known concentrations and corrected by the protein content.

### 2.13. Delta Aminolevulinate Dehydratase (δ-ALA-D) activity assay

The enzyme was assayed as described previously (Sassa, 1982) by measuring the rate of product porphobilinogen (PBG) formation. After 10 min of pre-incubation with homogenized liver or total blood from treated mice at 37 °C, in a medium containing 100 mM potassium phosphate buffer, pH 6.8, the enzymatic reaction was initiated by adding the substrate aminolevulinic acid (ALA) to a final concentration of 2.5 mM. The incubation was carried out for 1 h, at 37 °C, and was stopped by adding 10% TCA containing 10 mM $HgCl_2$. The reaction product was determined using a modified Ehrlich's reagent at 555 nm, with a molar absorption coefficient of $6.1 \times 10^4$ for the Ehrlich porphobilinogen salt. The enzyme activity was expressed in percent of the control.

### 2.14. Glutathione peroxidases (GPx) assay.

GPx was determined as described previously (Paglia and Valentine, 1967). Tissue supernatants (200–400 μg protein) were added to the assay mixture consisting of 1 mM sodium azide, 1 mM GSH, 50 mM potassium phosphate (pH 7.0), and 0.1 unit of glutathione reductase. Reaction was started by the addition of hydrogen peroxide ($H_2O_2$) to give a final concentration of 0.4 mM. Conversion of NADPH to nicotinamide adenine dinucleotide phosphate ($NADP^+$) was monitored continuously at 340 nm for 2 min. GPx activity was expressed as nmol of NADPH oxidized per minute per milligram of protein, using an extinction coefficient $6.22 \times 10^6$ $M^{-1}$ $cm^{-1}$ for NADPH.

### 2.15. Non protein thiol measurement (NPSH)

To estimate GSH content we determined NPSH as follows: 500 μL of 10% TCA was added to 500 μL of either the S1 homogenates of liver, or kidney, or heart or brain. After centrifugation (4000*g* at 4 °C for 10 min), the protein pellet was discarded and free –SH were determined in the clear supernatant (which was previously neutralized with 0.1 M NaOH) according to Ellman (1959).

### 2.16. Cytotoxicity assays

#### 2.16.1. Percent of hemolysis in human red blood cells

The 5% suspension RBCs in PBS (pH 7.4) was incubated under air atmosphere at 37 °C for 240 min, into IBTC concentrations from 10 to 200 μM were added to the medium. The reaction mixture was shaken gently while being incubated at 37 °C. The extent of hemolysis was determined spectrophotometrically as described previously (Kuang et al., 1994). Briefly, aliquots of the reaction mixture were taken out at appropriate time intervals, diluted with NaCl (0.15 M), and centrifuged at 2000 rpm for 10 min to separate the RBCs. The percentage hemolysis was determined by measuring the absorbance of the supernatant at 540 nm and compared with that of complete hemolysis by treating the same RBC suspension with distilled water.

#### 2.16.2. MTT assay

Percent cytotoxicity of IBTC was assessed using the 3-(4,5-dimethylthiazol-2-yl)-2, 5-diphenyl tetrazolium bromide (MTT) assay as described previously (Mosmann, 1983). Briefly, Murine J774 macrophage-like cells ($1 \times 10^4$) were allowed to adhere for 24 h under high humid environment in 5% $CO_2$ at 37 °C in 96 well culture plates. Also human lymphocytes were freshly isolated as described previously (Böyum, 1968) and plated in 96-well flat bottom tissue culture plate at a concentration of $1 \times 10^5$ cells/well containing 200 μl of RPMI-1640 supplemented with 10% FCS tissue culture medium. Then, for the both type of cells, IBTC concentrations from 10 to 200 μM were added to the medium and incubated for 24 h. After the respective exposure, MTT (5 mg/ml of stock in PBS) was added (10 μl/well in 100 μl of cell suspension), and plates were incubated for 4 h. At the end of incubation period, 200 μl of DMSO was added to each well. The plates were kept on shaker for 5 min at room temperature and then read at 550 nm using FisherBiotech Microkinetics Reader BT 2000. Untreated sets were also run under identical conditions and served as basal control.

### 2.17. Cholinesterase's activity

#### 2.17.1. Preparation of erythrocyte ghosts and plasma

Hemoglobin-free erythrocyte ghosts were prepared as previously described (Worek et al., 2002) with minor modifications. Briefly, blood of non-fasted healthy voluntary donors was collected. Heparinised human blood was centrifuged (3000*g*, 10 min) and the plasma removed and kept to test butyrylcholinesterase activity. Erythrocytes were washed three times with two volumes of sodium/potassium phosphate buffer (0.1 M, pH 7.4). Then, the packed erythrocytes were diluted in 20 volumes of hypotonic sodium/potassium phosphate buffer (6.7 mM, pH 7.4) to facilitate the hemolysis, followed by centrifugation at 30,000*g* (30 min, 4 °C). The supernatant was removed and the pellet resuspended in hypotonic phosphate buffer. After two additional washing cycles, the pellet was resuspended in sodium/potassium phosphate buffer (0.1 M, pH 7.4), passed through one more centrifugation at 30,000*g* (30 min, 4 °C) and were kindly removed. Next, the AChE activity was adjusted to the original activity by appropriate dilution with phosphate buffer (0.1 M, pH 7.4). Aliquots of the erythrocyte ghosts were stored at −20 °C until use.

Hemoglobin content present in ghost membranes was measured at 540 nm as the cyano-met-Hb form, but no hemoglobin was detected.

#### 2.17.2. Measure of cholinesterases activity

Ghost erythrocyte acetylcholinesterase and human plasma butyrylcholinesterase activities were estimated by Ellman method (Ellman et al., 1961), using acetylthiocholine iodide as substrate. The rate of hydrolysis of acetylthiocholine iodide is measured at 412 nm through the release of the thiol compound that, when reacted with DTNB, produces the color-forming compound TNB. Whole blood AChE was measured by Ellman method (Ellman et al., 1961) with modifications (Worek et al., 1999a,b). For butyrylcholinesterase activity, the same protocol was used, but butyrylthiocoline iodide was used as the substrate.

#### 2.17.3. Reactivation/protection of OP-inhibited cholinesterase

Ghost erythrocyte acetylcholinesterase and human plasma butyrylcholinesterase were exposed to IBTC in two different assay conditions in order to identify a possible protective or a reactivation capacity of IBTC:

(a) Protection: the enzyme was exposed to methamidophos (MAP) 25 μM and IBTC (10–100 μM) at the same time into a total incubation period of 60 min.
(b) Reactivation: the enzyme was firstly exposed to MAP 25 μM by 10 min (estimated time before aging). After this, the IBTC (10–100 μM) tested was added into the medium and the incubation followed by 50 min (to perform an equal total incubation time period of 60 min). Enzyme activities were referred to control activity.

The different protocols aim to test the prophylactic and therapeutic effect of IBTC on MAP-induced AChE inhibition.

### 2.18. Protein determination

The protein content was determined as described previously (Lowry et al., 1951) using bovine serum albumin (BSA) as standard.

### 2.19. Molecular docking

Docking simulations of the oximes with *Mus musculus* AChE were carried out using AutoDock Vina 1.1.1 (Trott and Olson, 2010), followed by redocking with Autodock 4.0.1. The non-aged MAP-inhibited *Mus musculus* AChE obtained from the RCSB Protein Data Bank (http://www.rcsb.org/pdb/) was used as macromolecule (PDB code 2jge). IBTC was constructed using the program Avogadro 0.9 and their geometry were optimized with the MMFF 94 force field. Both ligand and macromolecule are previously prepared using AutoDock Tools (Morris et al., 2009) and Chimera 1.5 (Pettersen et al., 2004). All rotatable bonds within the ligands were allowed to rotate freely, and the receptor was considered rigid. The grid was centered on the active site of from AChE and the dimensions of the grid box were consisted of 30 Å × 22 Å × 30 Å points, with spacing of 1 Å. The exhaustiveness was set to 50. All other parameters were used as defaults. For the ligand docked, the conformation from the lowest binding free energy with inferred inhibitory reactivity was accepted as the best affinity model. The redocking calculation were carried out using Autodock 4.0.1, following method of Musilek et al. (2011). Briefly, a Lamarckian genetic algorithm (Amber force field) was used, and a population of 150 individuals and 2500,000 function evaluations were applied. The structure optimization was performed for 27,000 generations. Docking calculations were set to 100 runs. At the end of calculation, Autodock performed cluster analysis. The 3D affinity grid box was designed to include the full active and peripheral site of AChE. The number of grid points in the *x*-, *y*- and *z*-axes was 60, 60 and 60 with grid points separated by 0.253 Å. The conformations and interactions were analyzed using the programs Accelrys Discovery Studio Visualizer 2.5 and PyMOL (Seeliger and de Groot, 2010).

### 2.20. Statistical analysis

Data are expressed as means ± SEM. Statistical analysis was performed using one-way analysis of variance (ANOVA), followed by Student–Newman–Keuls test when appropriate. In addition, linear regression was performed to identify a possible dose dependent effect. Values of $p < 0.05$ were considered significant.

## 3. Results

### 3.1. Ex vivo toxicology screening

Table 1 shows that IBTC did not significantly affect DCF-RS levels in tissue homogenates. In addition, lipid peroxidation, indicated by TBARS levels (Table 2), did not change significantly in liver, kidney, or brain homogenates after treatment with any concentration of IBTC. However, there was a significant reduction in TBARS level in heart homogenates after treatment with most of the concentrations of IBTC. NPSH levels did not change in liver, kidney,

**Table 1**
Effect of IBTC treatment on DCF-RS levels on liver, kidney, heart and brain homogenates.

| | DCF-RS levels (Mean ± SEM) | | | |
|---|---|---|---|---|
| | Liver | Kidney | Heart | Brain |
| Control | 100.00 ± 0.95 | 100.00 ± 1.13 | 100.00 ± 2.26 | 100.00 ± 1.08 |
| 1 mg/kg | 115.73 ± 5.63 | 109.41 ± 0.72 | 88.4 ± 5.02 | 95.26 ± 6.21 |
| 10 mg/kg | 114.10 ± 4.98 | 104.91 ± 2.13 | 93.52 ± 6.15 | 92.04 ± 1.94 |
| 50 mg/kg | 107.24 ± 3.69 | 102.86 ± 1.32 | 110.08 ± 1.25 | 103.39 ± 2.54 |
| 100 mg/kg | 115.16 ± 5.68 | 101.41 ± 1.54 | 89.03 ± 4.51 | 80.10 ± 6.20 |
| 250 mg/kg | 121.09 ± 7.64 | 103.71 ± 3.37 | 99.82 ± 4.26 | 81.74 ± 5.76 |
| 500 mg/kg | 112.03 ± 4.97 | 100.14 ± 3.43 | 102.26 ± 5.49 | 91.20 ± 1.49 |

Data are expressed as percentage of the control. The values are expressed as mean ± SEM of four independent experiments in duplicate. Data were analyzed by analysis of variance (ANOVA), followed by Student–Newman–Keuls post hoc test. Values of $p < 0.05$ were considered significant.

**Table 2**
Effect of IBTC treatment on TBARS levels on liver, kidney, heart and brain homogenates.

| | TBARS levels (Mean ± SEM) | | | |
|---|---|---|---|---|
| | Liver | Kidney | Heart | Brain |
| Control | 100.00 ± 4.35 | 100.00 ± 1.18 | 100.00 ± 1.74 | 100.00 ± 4.86 |
| 1 mg/kg | 99.75 ± 17.49 | 95.66 ± 7.52 | 67.96 ± 8.93* | 111.17 ± 10.3 |
| 10 mg/kg | 84.10 ± 6.54 | 75.98 ± 6.95 | 58.41 ± 9.10* | 114.54 ± 5.90 |
| 50 mg/kg | 106.45 ± 12.08 | 69.07 ± 11.57 | 69.55 ± 10.25* | 80.48 ± 7.82 |
| 100 mg/kg | 120.95 ± 11.09 | 96.60 ± 12.91 | 61.24 ± 2.67* | 86.30 ± 7.83 |
| 250 mg/kg | 115.83 ± 7.76 | 94.09 ± 10.21 | 65.99 ± 9.99* | 76.64 ± 10.53 |
| 500 mg/kg | 118.91 ± 1.27 | 89.91 ± 3.29 | 81.65 ± 8.06 | 92.44 ± 5.93 |

Data are expressed as percentage of the control. The values are expressed as mean ± SEM of four independent experiments in duplicate. Data were analyzed by analysis of variance (ANOVA), followed by Student–Newman–Keuls post hoc test. Values of $p < 0.05$ were considered significant.
* Indicates statistical difference from control group ($p < 0.05$).

**Table 3**
Effect of IBTC treatment on NPSH levels on liver, kidney, heart, brain homogenates.

| | NPSH levels (Mean ± SEM) | | | |
|---|---|---|---|---|
| | Liver | Kidney | Heart | Brain |
| Control | 100.00 ± 0.61 | 100.00 ± 4.44 | 100.00 ± 2.92 | 100.00 ± 1.55 |
| 1 mg/kg | 91.09 ± 5.22 | 133.30 ± 15.22 | 90.44 ± 5.67 | 125.79 ± 1.01 |
| 10 mg/kg | 91.90 ± 15.14 | 111.93 ± 12.46 | 86.15 ± 7.00 | 104.61 ± 1.45 |
| 50 mg/kg | 95.78 ± 2.25 | 154.59 ± 14.39 | 100.35 ± 11.38 | 108.69 ± 7.67 |
| 100 mg/kg | 83.00 ± 8.33 | 131.21 ± 6.53 | 97.49 ± 13.59 | 159.13 ± 14.13* |
| 250 mg/kg | 96.67 ± 13.73 | 133.16 ± 9.94 | 96.81 ± 10.75 | 186.15 ± 28.37* |
| 500 mg/kg | 98.75 ± 2.27 | 135.65 ± 16.61 | 113.22 ± 8.56 | 176.34 ± 12.24* |

Data are expressed as percentage of the control. The values are expressed as mean ± SEM of four independent experiments in duplicate. Data were analyzed by analysis of variance (ANOVA), followed by Student–Newman–Keuls post hoc test. Values of $p < 0.05$ were considered significant.
* Indicates statistical difference from control group ($p < 0.05$).

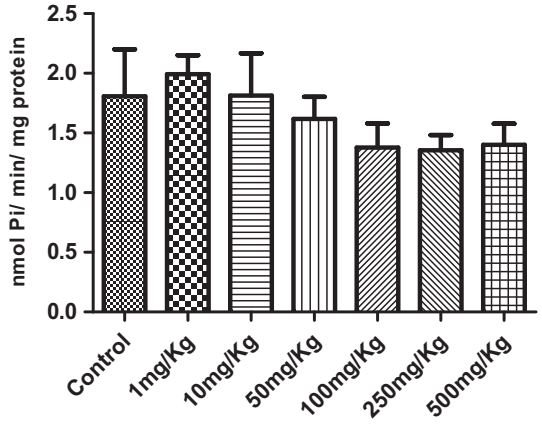


**Fig. 2.** Effect of IBTC treatment on $Na^+/K^+$ ATPase activity on brain homogenate. $Na^+/K^+$ ATPase activity is expressed as nmol Pi/min/mg protein. The values are expressed as mean ± SEM of four independent experiments in duplicate. Data were analyzed by analysis of variance (ANOVA), followed by Student–Newman–Keuls post hoc test. Values of $p < 0.05$ were considered significant.

or heart homogenates, but increased significantly in brain homogenates after treatment with IBTC (Table 3). Catalase and GPx activities did not change significantly (data not shown). In addition, $Na^+/K^+$ ATPase activity in the brain (Fig. 2) and ALA-D activity in liver and blood (Fig. 3A and B) did not change significantly. In addition, $LD_{50}$ was considered higher than 500 mg/kg.

### 3.2. Cell viability

#### 3.2.1. Percent of hemolysis

The percent of hemolysis in RBCs in the presence of various concentrations (10–200 μM) of IBTC did not change significantly compared to controls (data not shown).

#### 3.2.2. MTT assay

Murine J774 macrophage-like cells and isolated human lymphocytes were used to test the cytotoxicity of IBTC. Fig. 4 shows the MTT levels in these cell types. Concentrations of 50 μM of IBTC and above significantly reduced MTT levels compared to controls in J774 macrophage-like cells (Fig. 4A). The MTT levels did not change significantly compared to controls in isolated human lymphocytes (Fig. 4B).

### 3.3. Cholinesterase activity

MAP exposure at a concentration of 25 μM inhibited AChE and BChE activity in all samples. None of the IBTC concentrations tested had a significant effect on AChE or BChE activity (data not shown). No direct hydrolytic effect of IBTC on acetylthiocholine or butyrylthiocholine was observed (data not shown).

IBTC protected against MAP-inhibition of AChE and BChE in human erythrocyte ghosts (Fig. 5A and B). Treatment with MAP plus IBTC (at 10, 25, 50, and 100 μM) resulted in significantly increased cholinesterase activity compared to MAP alone (Fig. 5A and B). IBTC also significantly ($p < 0.05$) reactivated the AChE and BChE enzyme activities at concentrations of 10, 25, 50, and 100 μM (Fig. 6A and B) compared to MAP alone.

### 3.4. Molecular docking results

Since different enantiomers of methamidophos can bind to Ser203, Sp and Rp we performed docking studies with both Sp (SGX) and Rp (SGR) enantiomers of MAP-inhibited AChE from *Mus musculus* (PDB code: 2jge) (Fig. 7). In the Rp conformation of methamidophos, IBTC was located in the active site between the peripheral anionic site (PAS) (Tyr124) and the internal anionic site (Tyr341). The binding energy was −9.2 kcal/mol for the Rp enantiomer. The thiocarbonyl group was 7.707 angstroms from the

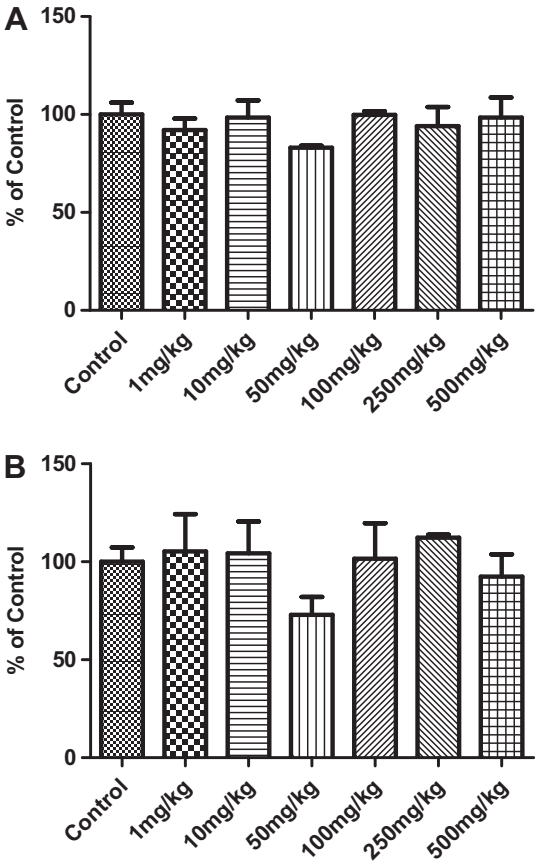


**Fig. 3.** Effect of IBTC treatment on Delta Aminolevulinate Dehydratase (δ-ALA-D) activity on liver (A) homogenate and on total blood (B). Data are expressed as percentage of the control. The values are expressed as mean ± SEM of four independent experiments in duplicate. Data were analyzed by analysis of variance (ANOVA), followed by Student–Newman–Keuls post hoc test. Values of $p < 0.05$ were considered significant.

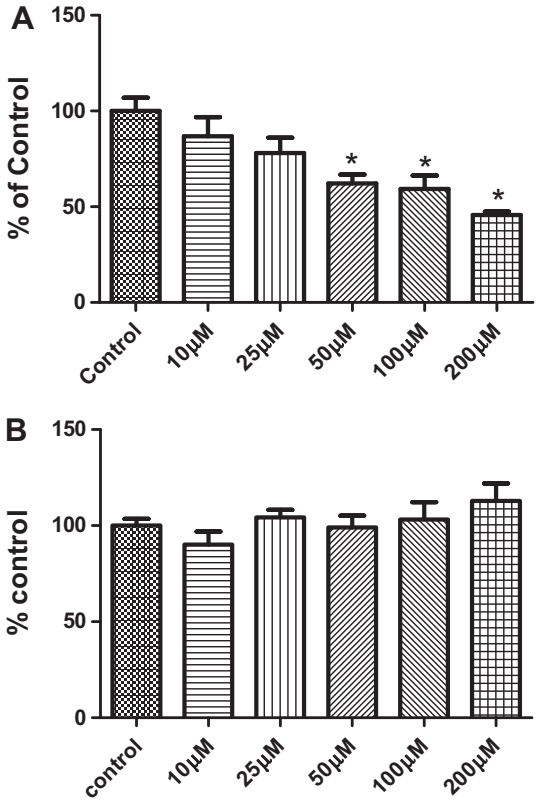


**Fig. 4.** Effect of IBTC on percent cytotoxicity (MTT assay) in Murine J774 macrophage-like cells (A) and in human isolated lymphocytes (B). Both types of cells were exposed to various concentrations of IBTC for 24 h prior to the addition of MTT for 4 h. The values are expressed as mean ± SEM of three independent experiments in triplicate. Data were analyzed by analysis of variance (ANOVA), followed by Student–Newman–Keuls post hoc test. Values of $p < 0.05$ were considered significant. * indicates statistical difference from control group ($p < 0.05$).

phosphate of SGR203, and the hydrazinic nitrogen of the thiosemicarbazone function was 2.873 Å from the carboxylic oxygen of residue Asp74 and 3.305 Å from the oxygen of residue Tyr341. The terminal thioamidic nitrogen hydrogen bonded with residue Tyr124 of the peripheral anionic site. The other fragment of the molecule was located close to the internal anionic site and stabilized by hydrogen bonds with residues Thr83 (nitrogen of the indole group) and Tyr337 (hydrogen bond with the amidic oxygen and the iminic nitrogen present on the thiosemicarbazone function). Only one cation–Pi interaction occurred between IBTC and the enzyme active site, which was between the aromatic ring from the terminal thioamidic function and phosphate of the SER203.

In the Sp conformation of methamidophos, similar to the Rp enantiomer of the serine modified by MAP, IBTC was stabilized in the active site between the peripheral anionic site (PAS) (Tyr124) and the internal anionic site (Tyr341). The binding energy was −8.95 kcal/mol. The thiocarbonyl group was 6.311 Å from the phosphate of SGX203 and the hydrazinic nitrogen of the thiosemicarbazone function was 2.818 Å from the carboxylic oxygen of residue Asp74 and 3.271 Å from the oxygen of residue Tyr341. In this conformation (SGX), the sulfur group was closer to the phosphate of the modified serine than in the SGR conformation. The aromatic ring from the terminal thioamidic function was stabilized in a hydrophobic region between the PAS (Tyr337 and Tyr341) and the acyl binding pocket (Phe338). The amidic oxygen formed a hydrogen bond with residue Tyr337 as well as with the iminic nitrogen. There was also a hydrogen bond between residue Thr87 and the iminic nitrogen. Pi interactions did not directly occur with the molecule.

## 4. Discussion

One purpose of our study was to investigate the potential toxic properties of IBTC, a compound that has been investigated in many biological models of oxidative stress. In our previous study (Barcelos et al., 2011) we demonstrated that this compound has high antiatherogenic potential. However, its toxicity to organisms as well as its possible action on cholinesterases had not been yet elucidated. In the present study we showed that subcutaneous injection of IBTC did not increase oxidative stress, had no impact on enzymes usually affected by pesticide compounds (Banerjee et al., 1999; Gultekin et al., 2000; Gupta et al., 2001), and did not induce alterations in several antioxidant enzymes (Tables 1–3; Figs. 2 and 3). In addition, our study clearly demonstrates that IBTC can protect and reactivate AChE and BChE inhibited by MAP (Figs. 5 and 6).

We investigated IBTC in vivo in order to determine whether it had any toxic effects in mice. We found that IBTC has low toxicity when administered by subcutaneous (s.c.) injection, with an $LD_{50}$ of higher than 500 mg/kg, and had no effect on body weight (data not shown). No cytotoxicity was detected in isolated human lymphocytes and only concentrations of 50 μM and higher lowered MTT levels in murine J774 macrophage-like cells. Moreover, the presence of IBTC did not change the percent of hemolysis in RBCs

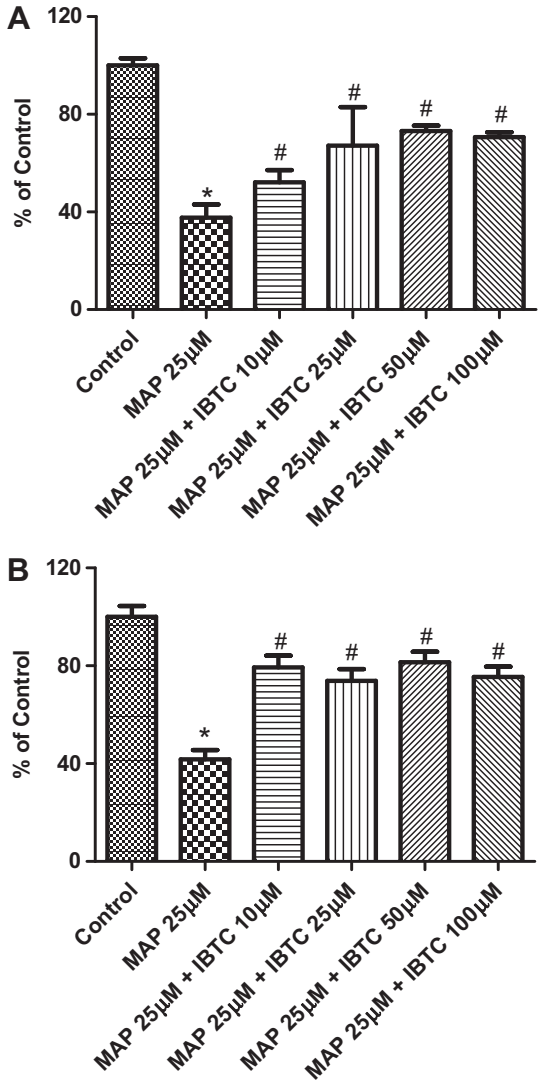


**Fig. 5.** Protective effect of IBTC on AChE activity from ghost erythrocytes (A) and BChE from plasma (B) on methamidophos (MAP) inhibition. IBTC was added to the reaction medium at the same time of methamidophos. The data are expressed as percentage from control group (100%) of five independent experiments in duplicate. Data were analyzed by analysis of variance (ANOVA), followed by Student–Newman–Keuls post hoc test. Values of $p < 0.05$ were considered significant. * indicates statistical difference from control group ($p < 0.05$) # indicates statistical difference from methamidophos 25 μM group ($p < 0.05$).

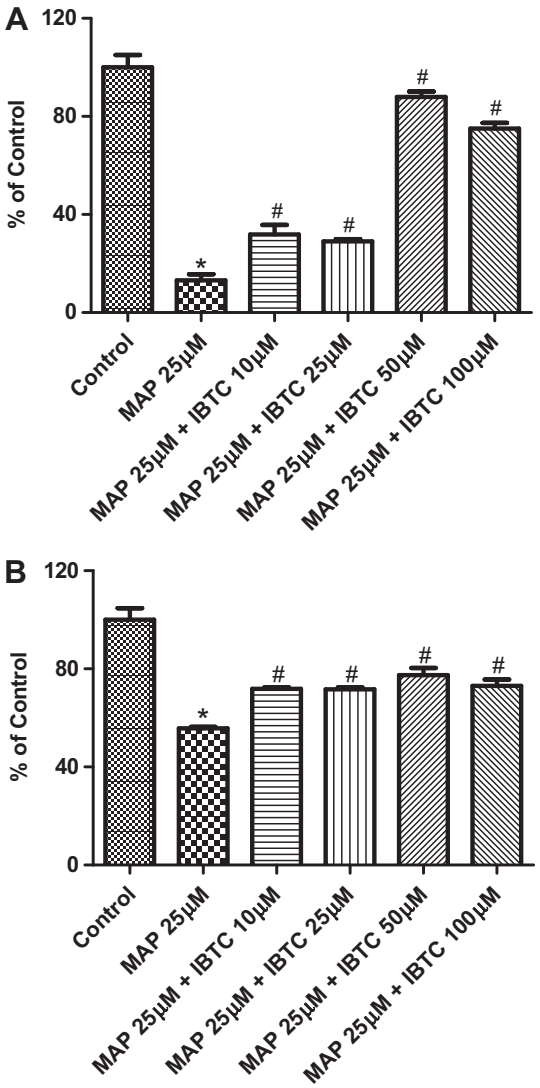


**Fig. 6.** Reactivation effect of IBTC on AChE activity from ghost erythrocytes (A) and BChE from plasma (B) on methamidophos (MAP) inhibition. IBTC was added 10 min after methamidophos in the reaction medium. The data are expressed as percentage from control group (100%) of five independent experiments in duplicate. Data were analyzed by analysis of variance (ANOVA), followed by Student–Newman–Keuls post hoc test. Values of $p < 0.05$ were considered significant. * indicates statistical difference from control group ($p < 0.05$) # indicates statistical difference from methamidophos 25 μM group ($p < 0.05$).

compared to controls. These results corroborate those of Puntel et al. (2009) who found that thiosemicarbazone-derived compounds have low toxicity.

Although we did not specifically measure RS formation, it is well known that excessive RS could not only induce DCF-RS formation but also contribute to the initiation of a complex cascade of reactions that culminates with lipid peroxidation (increase in TBARS levels). We demonstrated that IBTC did not change DFC-RS levels and did not increase lipid peroxidation, indicating that IBTC does not produce excessive RS itself or disrupt the cellular environment such that RS production increases. In addition, we found that there was no depletion in NPSH levels and no changes in catalase and GPx activities, indicating that there was no depletion or alteration of these antioxidant systems.

δ-ALA-D is an enzyme that catalyzes the condensation of two δ-aminolevulinic acid (ALA) molecules into porphobilinogen. Consequently, δ-ALA-D inhibition may impair heme biosynthesis (Jaffe, 1995) and can result in the accumulation of δ-ALA, which may affect aerobic metabolism and have some prooxidant activity (Bechara et al., 1993). Moreover, δ-ALA-D activity is a good marker of oxidative stress (Maciel et al., 2000) and can be inhibited by thiol oxidized radicals (Farina et al., 2001; Folmer et al., 2003). Here we demonstrated that there were no significant effects on δ-ALA-D activity, indicating that IBTC does not affect the essential –SH groups on the active site of the enzyme or increase oxidative stress.

$Na^+/K^+$-ATPase, a sulfhydryl-containing enzyme, is embedded in the cell membrane and is responsible for the active transport of sodium and potassium ions in the nervous system. Since $Na^+/K^+$-ATPase is crucial for maintaining ionic gradients in neurons (Xiong and Stringer, 2000), a reduction in the activity of this enzyme may affect neural activity and memory storage (Balk et al., 2010). Our study demonstrated that the $Na^+/K^+$-ATPase activity was not modified by IBTC at any of the concentrations tested, indicating that IBTC has no toxic properties to neurons. Previous reports have

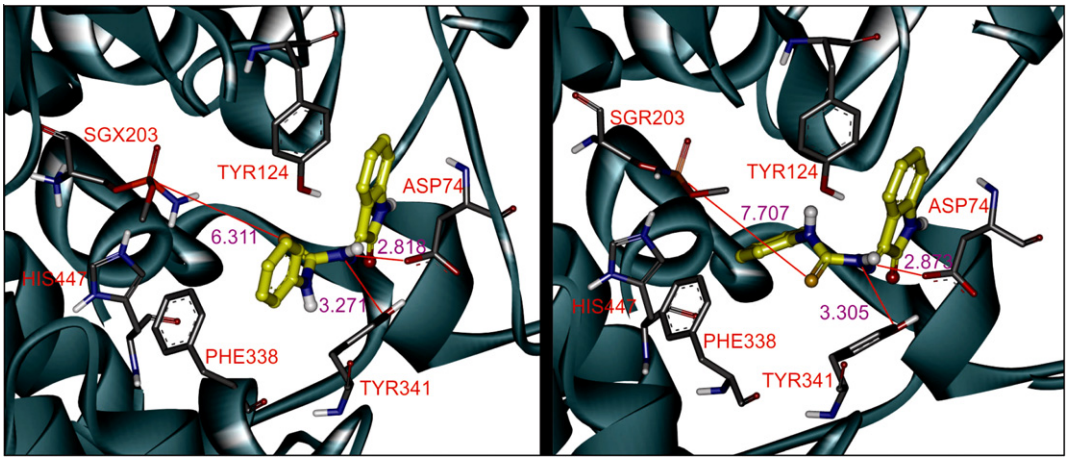


**Fig. 7.** Representative molecular models of IBTC binding the active site of *Mus musculus* AChE in the two different enantiomers for the methamidophos-modified Ser203: SGX (left panel) and SGR (right panel). Ligand is shown in ball-and-stick drawing, the carbons of the ligand is shown in yellow. (For interpretation of the references to colour in this figure legend, the reader is referred to the web version of this article.)

demonstrated the importance of thiol groups for $Na^+/K^+$-ATPase catalysis and –SH groups of this enzyme are highly susceptible to oxidizing agents (Bavaresco et al., 2003; de Assis et al., 2003). The unchanged NPSH levels found here are in agreement with the unchanged activities of ALA-D and $Na^+/K^+$-ATPase.

We also demonstrate that IBTC did not alter the activity of AChE and BChE, enzymes related to dysfunctions in the cholinergic neurotransmission (Mukherjee et al., 2007) and to systemic inflammatory conditions, such as diabetes mellitus, hypertension, insulin resistance, and hyperlipidemia (Das, 2007).

AChE and BChE are strongly related to the intoxications caused by pesticides and the implications of pesticides residues on human health have yet to be comprehensively documented. Pesticides may induce oxidative stress, leading to generation of free radicals and alterations in antioxidants, oxygen free radicals, scavenging enzyme systems, and lipid peroxidation. This way, after verifying that IBTC does not alter antioxidant systems and has no toxic effects, we tested the capacity of IBTC to protect and reactivate the activity of AChE and BChE after inhibition with MAP. In human erythrocyte ghost and in human plasma BChE, IBTC was able to protect and reactivate both enzymes from MAP inhibition at all concentrations tested (Figs. 5 and 6). The protective activity for AChE and BChE against MAP inhibition works via competitive inhibition.

Molecular docking results indicate that IBTC can enter the active site of AChE by binding to the peripheral anionic site (Trp134 and Tyr124) and internal anionic site (Thr83 and Tyr337), thus preventing MAP from accessing the catalytic residue Ser203 and protecting AChE and BChE from inhibition, and proving that IBTC cannot itself inhibit AChE or BChE, since in vitro tests demonstrate that the presence of IBTC on these sites do not affect AChE and BChE activities.

Our most interesting result is that IBTC can reactivate AChE and BChE after inhibition by MAP. As far as we know, there are few compounds that are not oximes that can reactivate AChE and BChE inhibited by OPs and there is no literature concerning the use of thiosemicarbazones against OP intoxication. In that way, our study demonstrates for the first time that a thiosemicarbazone derivate can protect and reactivate AChE and BChE from OP inhibition. The use of many different oximes, the classical therapy for OPs poisoning, is controversial since metabolic degradation of oximes can have deleterious effects, such as formation of toxic products such as hydrogen cyanide, and numerous side effects, including nausea, vomiting, dizziness, loss of consciousness, visual alterations, confusion, headache, tachycardia, neuromuscular blockage, and muscular weakness (Bardin et al., 1994; Carlton et al., 1998; Hardman et al., 1996). New and more effective drugs with fewer toxicological effects are necessary for cholinesterases reactivation.

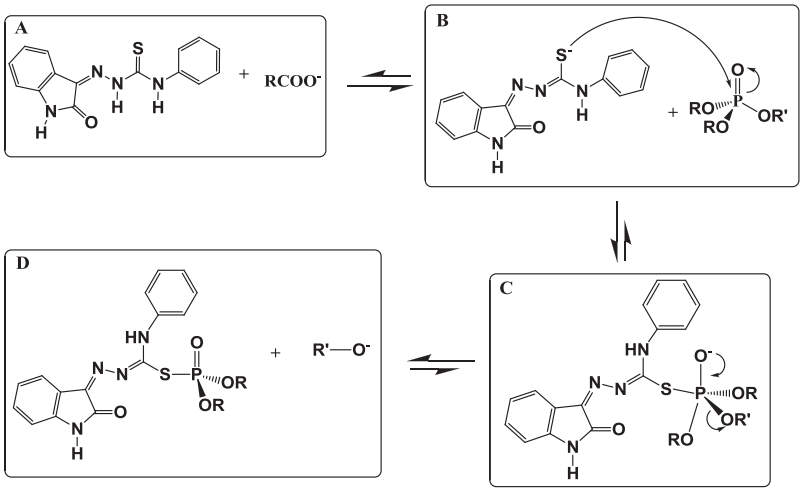


**Scheme 1.** Possible mechanism of IBTC reactivation on methamidophos-inhibited AChE.

In addition, oximes are weaker reactivators of BChE (Worek et al., 1999a,b), and IBTC can reactivate both AChE and BChE activities. The reactivation of BChE is very important, since BChE is a co-regulator of acetylcholine in brain (Giacobini, 2000) and replaces AChE in the maintenance of the structure and physiological integrity of the cholinergic system (Mesulam et al., 2002). Darvesh et al. (2004) also showed that BChE is highly active in the synaptic cleft in intrinsic cardiac neurons, helping to reduce high acetylcholine levels (Darvesh et al., 2004). IBTC seems to reactivate cholinesterases via its position at the peripheral anionic site and the acyl binding pocket, which is in agreement with previous results obtained for mono-oxime bisquaternary acetylcholinesterase reactivators (Musilek et al., 2011).

As illustrated in Scheme 1, we observed that the imino hydrogen (A) from IBTC can react with a carboxylate group ($RCOO^-$) of the Asp74 residue (the distance of the imino hydrogen of the IBTC and the $RCOO^-$ group of the enzyme is about 2.8 Å), which could lead to IBTC deprotonation and formation of an anionic intermediate (B). Then, a nucleophilic attack by the thiolate on the electrophilic center of methamidophos (B) can occur, which is the site of inhibition of the enzyme AChE (OR′). This intermediate has the phosphate group (P) penta coordinated (C), which causes methamidophos to leave the active site of the enzyme (OR′), reactivating the enzyme and releasing the phosphate group, which returns to the tetrahedral geometry bound only to IBTC (D). Based in this mechanism, the SGX, not the SGR, conformation of the MAP-inhibited AChE seems to be the more likely conformation to be reactivated since the sulfur group is positioned closer to the electrophilic attack site (OP moiety in the modified Ser203). This is in agreement with previous work that showed that Sp enantiomers (SGX conformation) of methylphosphonate esters are more reactive in forming the conjugate with the enzyme and the rates of reactivation by oximes also indicate a preference of Sp over Rp (Wong et al., 2000).

## 5. Conclusion

The thiosemicarbazone derived compound, IBTC, besides acting like an antioxidant and antiatherogenic (Barcelos et al., 2011), has low toxicity and does not alter the antioxidant system. We have demonstrated for the first time that a thiosemicarbazone derivate can protect AChE and BChE from MAP intoxication by preventing MAP binding at the active site of the enzymes and can also reactivate AChE and BChE activities by interacting with MAP and releasing the active site. Future studies are needed to test IBTC against intoxication by other OPs and also evaluate its efficacy after long-term exposure to MAP. However, our work indicates that IBTC may be a useful therapeutic compound for MAP intoxication.

## Conflict of interest

The authors declare that there are no conflicts of interest.

## Acknowledgements

Work supported by the FINEP research grant "Rede Instituto Brasileiro de Neurociência (IBN-Net)" # 01.06.0842-00. INCT – National Institute of Science and Technology for Excitotoxicity and Neuroprotection/CNPq also supported this work. F.A.A.S. and N.B.V.B. received a fellowship from CNPq. R.P.B., T.H.L. and G.P.A. received a fellowship from CAPES.

## References

Abdollahi, M., Ranjbar, A., Shadnia, S., Nikfar, S., Rezaie, A., 2004. Pesticides and oxidative stress: a review. Med. Sci. Monit. 10 (6), RA141–RA147.

Aebi, H., 1984. Catalase in vitro. Methods Enzymol. 105, 121–126.

Ashani, Y., Radić, Z., Tsigelny, I., Vellom, D.C., Pickering, N.A., Quinn, D.M., Doctor, B.P., Taylor, P., 1995. Amino acid residues controlling reactivation of organophosphonyl conjugates of acetylcholinesterase by mono- and bisquaternary oximes. J. Biol. Chem. 270 (11), 6370–6380.

Atkinson, A., Gatenby, A.D., Lowe, A.G., 1973. The determination of inorganic orthophosphate in biological systems. Biochim. Biophys. Acta 320 (1), 195–204.

Balk, R.e.S., Bridi, J.C., Portella, R.e.L., Carvalho, N.R., Dobrachinski, F., da Silva, M.H., Amaral, G.P., Dias, G.R., Barbosa, N.e.V., Soares, F.A., 2010. Clomipramine treatment and repeated restraint stress alter parameters of oxidative stress in brain regions of male rats. Neurochem. Res. 35 (11), 1761–1770.

Banerjee, B.D., Seth, V., Bhattacharya, A., Pasha, S.T., Chakraborty, A.K., 1999. Biochemical effects of some pesticides on lipid peroxidation and free-radical scavengers. Toxicol. Lett. 107 (1–3), 33–47.

Barcelos, R.P., de Lima Portella, R., da Rosa, E.J., Fonseca, A.e.S., Bresolin, L., Carratu, V., Soares, F.A., Barbosa, N.V., 2011. Thiosemicarbazone derivate protects from AAPH and Cu(2+)-induced LDL oxidation. Life Sci. 89 (1–2), 20–28.

Bardin, P.G., van Eeden, S.F., Moolman, J.A., Foden, A.P., Joubert, J.R., 1994. Organophosphate and carbamate poisoning. Arch. Intern. Med. 154 (13), 1433–1441.

Bavaresco, C.S., Calcagnotto, T., Tagliari, B., Delwing, D., Lamers, M.L., Wannmacher, C.M., Wajner, M., Wyse, A.T., 2003. Brain Na+, K(+)-ATPase inhibition induced by arginine administration is prevented by vitamins E and C. Neurochem. Res. 28 (6), 825–829.

Bechara, E., Medeiros, M., Monteiro, H., 1993. A free radical hypothesis of lead poisoning and inborn porphyrias associated with 5-aminolevulinic acid overload. Quim. Nova 16, 7.

Beraldo, H., Gambino, D., 2004. The wide pharmacological versatility of semicarbazones, thiosemicarba-zones and their metal complexes. Mini Rev. Med. Chem. 4 (1), 31–39.

Bourne, Y., Taylor, P., Marchot, P., 1995. Acetylcholinesterase inhibition by fasciculin: crystal structure of the complex. Cell 83 (3), 503–512.

Böyum, A., 1968. Isolation of mononuclear cells and granulocytes from human blood. Isolation of monuclear cells by one centrifugation, and of granulocytes by combining centrifugation and sedimentation at 1 g. Scand. J. Clin. Lab. Invest. Suppl. 97, 77–89.

Carlton, F.B., Simpson, W.M., Haddad, L.M., 1998. The organophosphate and other insecticides. In: Clinical Management of Poisoning and Drug Overdose. W.S. Company, Philadelphia, Pensylvania, USA, pp. 836–850.

da Silva, A.P., Farina, M., Franco, J.L., Dafre, A.L., Kassa, J., Kuca, K., 2008. Temporal effects of newly developed oximes (K027, K048) on malathion-induced acetylcholinesterase inhibition and lipid peroxidation in mouse prefrontal cortex. Neurotoxicology 29 (1), 184–189.

da Silva, A.P., Meotti, F.C., Santos, A.R., Farina, M., 2006. Lactational exposure to malathion inhibits brain acetylcholinesterase in mice. Neurotoxicology 27 (6), 1101–1105.

Darvesh, S., Arora, R.C., Martin, E., Magee, D., Hopkins, D.A., Armour, J.A., 2004. Cholinesterase inhibitors modify the activity of intrinsic cardiac neurons. Exp. Neurol. 188 (2), 461–470.

Das, U.N., 2007. Acetylcholinesterase and butyrylcholinesterase as possible markers of low-grade systemic inflammation. Med. Sci. Monit. 13 (12), RA214–RA221.

de Assis, D.R., Ribeiro, C.A., Rosa, R.B., Schuck, P.F., Dalcin, K.B., Vargas, C.R., Wannmacher, C.M., Dutra-Filho, C.S., Wyse, A.T., Briones, P., Wajner, M., 2003. Evidence that antioxidants prevent the inhibition of Na+, K(+)-ATPase activity induced by octanoic acid in rat cerebral cortex in vitro. Neurochem. Res. 28 (8), 1255–1263.

Ekström, F., Akfur, C., Tunemalm, A.K., Lundberg, S., 2006. Structural changes of phenylalanine 338 and histidine 447 revealed by the crystal structures of tabun-inhibited murine acetylcholinesterase. Biochemistry 45 (1), 74–81.

Ellman, G.L., 1959. Tissue sulfhydryl groups. Arch. Biochem. Biophys. 82 (1), 70–77.

Ellman, G.L., Courtney, K.D., Andres Jr., V., Feather-Stone, R.M., 1961. A new and rapid colorimetric determination of acetylcholinesterase activity. Biochem. Pharmacol. 7, 88–95.

Farina, M., Folmer, V., Bolzan, R.C., Andrade, L.H., Zeni, G., Braga, A.L., Rocha, J.B., 2001. Selenoxides inhibit delta-aminolevulinic acid dehydratase. Toxicol. Lett. 119 (1), 27–37.

Folmer, V., Soares, J.C., Gabriel, D., Rocha, J.B., 2003. A high fat diet inhibits delta-aminolevulinate dehydratase and increases lipid peroxidation in mice (*Mus musculus*). J. Nutr. 133 (7), 2165–2170.

Fonseca, A.d.S., Peres, G.L., Storino, T.G., Bresolin, L., Carratu, V.S., Giglio, V.F., Crespan, E.d.R., Manfredo, H., 2010. Synthesis and structural characterization of the ligand isatin-3-($N^4$-benzylthiosemicarbazone) and its mercury(II) complex. Quim. Nova 33, 1453–1456.

Giacobini, E., 2000. Cholinesterase and Cholinesterases Inhibitors. From Molecular Biology to Therapy, vol. 46. Martin Dunitz Publishers, London, pp. 181–226.

Grosfeld, H., Barak, D., Ordentlich, A., Velan, B., Shafferman, A., 1996. Interactions of oxime reactivators with diethylphosphoryl adducts of human acetylcholinesterase and its mutant derivatives. Mol. Pharmacol. 50 (3), 639–649.

Gultekin, F., Ozturk, M., Akdogan, M., 2000. The effect of organophosphate insecticide chlorpyrifos-ethyl on lipid peroxidation and antioxidant enzymes (in vitro). Arch. Toxicol. 74 (9), 533–538.

Gupta, R.C., Milatovic, D., Dettbarn, W.D., 2001. Depletion of energy metabolites following acetylcholinesterase inhibitor-induced status epilepticus: protection by antioxidants. Neurotoxicology 22 (2), 271–282.

Hardman, J.G., Gilman, A.G., Limbird, L.E., 1996. Anthicholinesterase agents. In: The Pharmacological Basis of Therapeutics. Goodman & Gilman's, pp. 161–176.

Holmstedt, B., 1959. Pharmacology of organophosphorus cholinesterase inhibitors. Pharmacol. Rev. 11, 567–688.
Jaffe, E.K., 1995. Porphobilinogen synthase, the first source of heme's asymmetry. J. Bioenerg. Biomembr. 27 (2), 169–179.
Kovarik, Z., Radić, Z., Berman, H.A., Simeon-Rudolf, V., Reiner, E., Taylor, P., 2004. Mutant cholinesterases possessing enhanced capacity for reactivation of their phosphonylated conjugates. Biochemistry 43 (11), 3222–3229.
Kryger, G., Silman, I., Sussman, J.L., 1998. Three-dimensional structure of a complex of E2020 with acetylcholinesterase from Torpedo californica. J. Physiol. Paris 92 (3–4), 191–194.
Kuang, Z.H., Wang, P.F., Zheng, R.L., Liu, Z.L., Liu, Y.C., 1994. Making vitamin C lipo-soluble enhances its protective effect against radical induced hemolysis of erythrocytes. Chem. Phys. Lipids 71 (1), 95–97.
Lowry, O., Roserbrough, N., Farr, A., Randall, R., 1951. Protein measurement with the Folin phenol reagent. J. Biol. Chem. 193 (1), 265–275.
Maciel, E.N., Bolzan, R.C., Braga, A.L., Rocha, J.B., 2000. Diphenyl diselenide and diphenyl ditelluride differentially affect delta-aminolevulinate dehydratase from liver, kidney, and brain of mice. J. Biochem. Mol. Toxicol. 14 (6), 310–319.
Marrs, T.C., 1993. Organophosphate poisoning. Pharmacol. Ther. 58 (1), 51–66.
Mesulam, M.M., Guillozet, A., Shaw, P., Levey, A., Duysen, E.G., Lockridge, O., 2002. Acetylcholinesterase knockouts establish central cholinergic pathways and can use butyrylcholinesterase to hydrolyze acetylcholine. Neuroscience 110 (4), 627–639.
Morris, G.M., Huey, R., Lindstrom, W., Sanner, M.F., Belew, R.K., Goodsell, D.S., Olson, A.J., 2009. AutoDock4 and AutoDockTools4: automated docking with selective receptor flexibility. J. Comput. Chem. 30 (16), 2785–2791.
Mosmann, T., 1983. Rapid colorimetric assay for cellular growth and survival: application to proliferation and cytotoxicity assays. J. Immunol. Methods 65 (1–2), 55–63.
Mukherjee, P.K., Kumar, V., Mal, M., Houghton, P.J., 2007. Acetylcholinesterase inhibitors from plants. Phytomedicine 14 (4), 289–300.
Musilek, K., Komloova, M., Holas, O., Horova, A., Pohanka, M., Gunn-Moore, F., Dohnal, V., Dolezal, M., Kuca, K., 2011. Mono-oxime bisquaternary acetylcholinesterase reactivators with prop-1,3-diyl linkage-preparation, in vitro screening and molecular docking. Bioorg. Med. Chem. 19 (2), 754–762.
Muszbek, L., Szabó, T., Fésüs, L., 1977. A high sensitive method for the measurement of ATPase activity. Anal. Biochem. 77 (1), 286–288.
Myhre, O., Andersen, J.M., Aarnes, H., Fonnum, F., 2003. Evaluation of the probes 2′,7′-dichlorofluorescin diacetate, luminol, and lucigenin as indicators of reactive species formation. Biochem. Pharmacol. 65 (10), 1575–1582.
Ohkawa, H., Ohishi, N., Yagi, K., 1979. Assay for lipid peroxides in animal tissues by thiobarbituric acid reaction. Anal. Biochem. 95 (2), 351–358.
Paglia, D.E., Valentine, W.N., 1967. Studies on the quantitative and qualitative characterization of erythrocyte glutathione peroxidase. J. Lab. Clin. Med. 70 (1), 158–169.
Pérez-Severiano, F., Rodríguez-Pérez, M., Pedraza-Chaverrí, J., Maldonado, P.D., Medina-Campos, O.N., Ortíz-Plata, A., Sánchez-García, A., Villeda-Hernández, J., Galván-Arzate, S., Aguilera, P., Santamaría, A., 2004. S-Allylcysteine, a garlic-derived antioxidant, ameliorates quinolinic acid-induced neurotoxicity and oxidative damage in rats. Neurochem. Int. 45 (8), 1175–1183.
Pettersen, E.F., Goddard, T.D., Huang, C.C., Couch, G.S., Greenblatt, D.M., Meng, E.C., Ferrin, T.E., 2004. UCSF Chimera – a visualization system for exploratory research and analysis. J. Comput. Chem. 25 (13), 1605–1612.
Puntel, G.O., Carvalho, N.R., Amaral, G.P., Lobato, L.D., Silveira, S.O., Daubermann, M.F., Barbosa, N.V., Rocha, J.B., Soares, F.A., 2011. Therapeutic cold: an effective kind to modulate the oxidative damage resulting of a skeletal muscle contusion. Free Radic. Res. 45 (2), 125–138.
Puntel, G.O., de Carvalho, N.R., Gubert, P., Palma, A.S., Dalla Corte, C.L., Avila, D.S., Pereira, M.E., Carratu, V.S., Bresolin, L., da Rocha, J.B., Soares, F.A., 2009. Butane-2,3-dionethiosemicarbazone: an oxime with antioxidant properties. Chem. Biol. Interact. 177 (2), 153–160.
Sassa, S., 1982. Delta-aminolevulinic acid dehydratase assay. Enzyme 28 (2–3), 133–145.
Seeliger, D., de Groot, B.L., 2010. Ligand docking and binding site analysis with PyMOL and Autodock/Vina. J. Comput. Aided Mol. Des. 24 (5), 417–422.
Sussman, J.L., Harel, M., Frolow, F., Oefner, C., Goldman, A., Toker, L., Silman, I., 1991. Atomic structure of acetylcholinesterase from Torpedo californica: a prototypic acetylcholine-binding protein. Science 253 (5022), 872–879.
Taylor, P., Radic, Z., Hosea, N.A., Camp, S., Marchot, P., Berman, H.A., 1995. Structural bases for the specificity of cholinesterase catalysis and inhibition. Toxicol. Lett. 82–83, 453–458.
Tomlin, C., (1994). The Pesticide Manual, A World Compendium. Croydon, British Crop Protection Council.
Trott, O., Olson, A.J., 2010. AutoDock Vina: improving the speed and accuracy of docking with a new scoring function, efficient optimization, and multithreading. J. Comput. Chem. 31 (2), 455–461.
Verma, R.S., Srivastava, N., 2001. Chlorpyrifos induced alterations in levels of thiobarbituric acid reactive substances and glutathione in rat brain. Indian J. Exp. Biol. 39 (2), 174–177.
Wada, K., Fujibayashi, Y., Yokoyama, A., 1994. Copper(II)[2,3-butanedionebis(N4-methylthiosemicarbazone)], a stable superoxide dismutase-like copper complex with high membrane penetrability. Arch. Biochem. Biophys. 310 (1), 1–5.
WHO, 1993. Methamidophos Health and Safety Guide. Geneva, World Health Organization.
Wong, L., Radic, Z., Brüggemann, R.J., Hosea, N., Berman, H.A., Taylor, P., 2000. Mechanism of oxime reactivation of acetylcholinesterase analyzed by chirality and mutagenesis. Biochemistry 39 (19), 5750–5757.
Worek, F., Aurbek, N., Koller, M., Becker, C., Eyer, P., Thiermann, H., 2007. Kinetic analysis of reactivation and aging of human acetylcholinesterase inhibited by different phosphoramidates. Biochem. Pharmacol. 73 (11), 1807–1817.
Worek, F., Diepold, C., Eyer, P., 1999a. Dimethylphosphoryl-inhibited human cholinesterases: inhibition, reactivation, and aging kinetics. Arch. Toxicol. 73 (1), 7–14.
Worek, F., Mast, U., Kiderlen, D., Diepold, C., Eyer, P., 1999b. Improved determination of acetylcholinesterase activity in human whole blood. Clin. Chim. Acta 288 (1–2), 73–90.
Worek, F., Reiter, G., Eyer, P., Szinicz, L., 2002. Reactivation kinetics of acetylcholinesterase from different species inhibited by highly toxic organophosphates. Arch. Toxicol. 76 (9), 523–529.
Worek, F., Thiermann, H., Szinicz, L., Eyer, P., 2004. Kinetic analysis of interactions between human acetylcholinesterase, structurally different organophosphorus compounds and oximes. Biochem. Pharmacol. 68 (11), 2237–2248.
Xiong, Z.Q., Stringer, J.L., 2000. Sodium pump activity, not glial spatial buffering, clears potassium after epileptiform activity induced in the dentate gyrus. J. Neurophysiol. 83 (3), 1443–1451.
Zayed, S.M., Fakhr, I.M., el-Magraby, S., 1984. Some toxicological aspects of methamidophos exposure in mice. J. Environ. Sci. Health B 19 (4–5), 467–478.